

Effects of surface topology on the formation of oxide islands on Cu surfaces

Guangwen Zhou,^{a)} Liang Wang, and Judith C. Yang

Department of Materials Science and Engineering, University of Pittsburgh, Pittsburgh, Pennsylvania 15261

(Received 6 May 2004; accepted 17 December 2004; published online 7 March 2005)

We examined the effects of surface topology on the nucleation and growth of Cu₂O oxide islands during the initial oxidation stages of Cu(100) and Cu(110) surfaces by *in situ* ultrahigh vacuum transmission electron microscopy and *ex situ* atomic force microscopy. Our observations indicate that nucleation of three dimensional oxide islands on single crystal surfaces is homogenous, surface defects and dislocations play a very limited role as preferential sites for oxide nucleation. On the other hand, grain boundaries are the preferential sites for oxide nucleation and the oxide islands formed along the grain boundaries show a faster growth rate than that on flat Cu surface. The oxidation on the faceted Cu(110) surface results in heterogeneous nucleation of oxide islands in the facet valleys and one-dimensional growth along the intersection direction of the facets. © 2005 American Institute of Physics. [DOI: 10.1063/1.1861147]

I. INTRODUCTION

The fundamental understanding of metal oxidation is of significant practical importance because one of the most essential properties of engineered metals is their corrosion resistance. Oxidation is also important for some thin film growth, such as ferroelectrics. The general sequence of the oxidation reaction on a clean metal surface is oxygen chemisorption, nucleation and growth of oxide, and bulk oxide growth. Surface science studies have provided many elegant insights into the atomic mechanisms of oxygen chemisorption but are limited to a few monolayers. In contrast, both low and high temperature bulk oxidation studies have focused on the growth of the thermodynamically stable oxide layer at the later stages of oxidation where the surface conditions were not generally well controlled. Hence, the least well-understood regime in metal oxidation is the nucleation and initial growth of oxides. One particularly interesting question is the role of surface defects and topology, such as dislocations, grain boundaries, surface steps and facets, in the initial oxide formation. Previous investigators have shown that surface defects do not seem to affect the oxidation of Si(111) surfaces.^{1,2} In contrast, the oxidation of Ge(111) seems to start at defect sites such as surface steps and vacancies.^{3,4} Concerning metal oxidation, conflicting results exist as to whether the oxide nucleates at defects.⁵⁻⁸ Milne and Howie⁹ proposed that surface steps play a significant role in the nucleation of copper oxides during oxidation of Cu(110) but were not able to observe the nucleation at these steps. Yet, Yang *et al.*¹⁰ revealed by *in situ* ultra high vacuum (UHV) transmission electron microscopy (TEM) that surface steps play only a limited role during the oxidation of Cu(100). Because of the existing contradiction in the literature and limited information of oxidation experiments carried out with well-controlled surface conditions, we per-

form a systematic investigation of the role of Cu orientations, Cu(100) and Cu(110), and defects on the oxide nucleation processes using *in situ* UHV-TEM, which permits visualization of structural changes at the nanometer scale during the oxidation processes in real time. By combining this with *ex situ* atomic force microscopy (AFM), we investigate the effects of surface topology, including surface indentations, dislocations, grain boundaries, as well as faceted surfaces, on the nucleation and growth of oxide islands during the initial oxidation stages of Cu(100) and Cu(110) surfaces.

II. EXPERIMENTS

Single crystal Cu(100) and Cu(110) films were grown on irradiated (100) and (110) NaCl substrates in an UHV e-beam evaporator system, where the base pressure was 10⁻¹⁰ Torr. 800 Å thick copper films were examined so that the film was thin enough to be examined by TEM, but thick enough for the initial oxidation behavior to be similar to that of bulk metal. The copper film was removed from the NaCl substrate by floatation in deionized water, washed and mounted on a specially prepared Si mount, where the modified microscope specimen holder allows for resistive heating of the specimen up to 1000 °C. The microscope used for this experiment is a modified JEOL-200CX. These modifications permit the introduction of gases directly into the microscope column and *in situ* heating. An UHV chamber was attached to the middle of the column, where the base pressure is ~10⁻⁸ Torr without the use of the helium cryoshroud. For more details about the experimental apparatus, see McDonald *et al.*¹¹ The microscope was operated at 100 keV to minimize irradiation effects. To oxidize the Cu film, oxygen gas (99.999% purity) was introduced into the TEM chamber with controllable oxygen partial pressure.

After removal from the Cu growth chamber, the copper film formed a native oxide on the surface due to exposure to air. To remove the native oxide from the Cu surface before

^{a)}Present address: Materials Science Division, Argonne National Laboratory, 9700 South Cass Avenue, Building 212, Argonne, Illinois 60439.

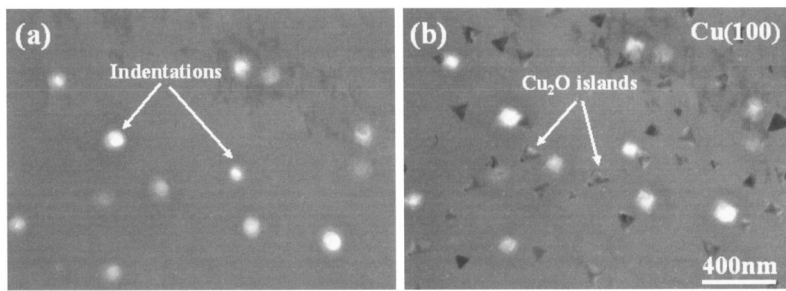


FIG. 1. (a) Bright field image of the Cu (100) film after the reduction of the oxide islands by methanol gas at 350 °C; (b) the same Cu surface area after *in situ* oxidation at 350 °C and oxygen pressure of 5×10^{-4} Torr.

the *in situ* oxidation experiments, the film is annealed inside the TEM in methanol vapor at 5×10^{-5} Torr for ~ 30 min, where the methanol reacts with the Cu_2O to form methoxy (CH_3O) and upon heating, forms gaseous CH_2O , CO , and CO_2 , which go into environment. The Cu film is then annealed *in situ* at ~ 800 °C under the vacuum of $\sim 6 \times 10^{-8}$ Torr. This high temperature annealing step is very effective to produce flat Cu surfaces and to remove impurities and carbon build-up on the Cu surface. The copper film is then cooled down to the desired temperature for the *in situ* oxidation experiments. To remove the copper oxide formed due to the *in situ* oxidation, the specimen is annealed at 350 °C and methanol gas was leaked into the TEM column again at a pressure of 5×10^{-5} Torr. After *in situ* oxidation/reduction, the samples are removed from the microscope and taken to a tapping atomic force microscope (AFM) for *ex situ* characterization of the topology of both the surface structure and oxide nanostructures.

III. RESULTS AND DISCUSSION

The *in situ* oxidation of the copper films results in the formation of epitaxial Cu_2O islands on the Cu surface, with cube on cube orientation, and it has been confirmed that the

oxide islands on the Cu surface show the three-dimensional (3D) growth mode, i.e., the oxide islands simultaneously increase the amount of the embedding into the copper substrate with their lateral growth during the continuous oxidation.^{12–16} Therefore, the subsequent removal of these oxide islands by *in situ* methanol reduction reaction creates indentations on the copper surfaces at the original oxide positions. Figure 1(a) is a bright field (BF) TEM micrograph showing the Cu(100) surface after the *in situ* removal of the oxide islands by methanol vapor at 350 °C, where the regions with the indentations show bright contrast in the BF TEM image because these regions are thinner than the surrounding Cu film. Figure 1(b) is the BF TEM micrograph of this Cu film from the same surface after a 7 min oxidation by leaking oxygen gas into the chamber at an oxygen pressure of $\sim 5 \times 10^{-4}$ Torr and the temperature of ~ 350 °C. The Cu_2O islands formed during the second *in situ* oxidation had a random distribution on the surface and the indentations were clearly not the preferential nucleation sites.

To obtain a better view of the shape of the indentation, the surface topology of the Cu films before and after the second oxidation was further examined by *ex situ* AFM. Figure 2 shows the AFM images of the details of the Cu(100)

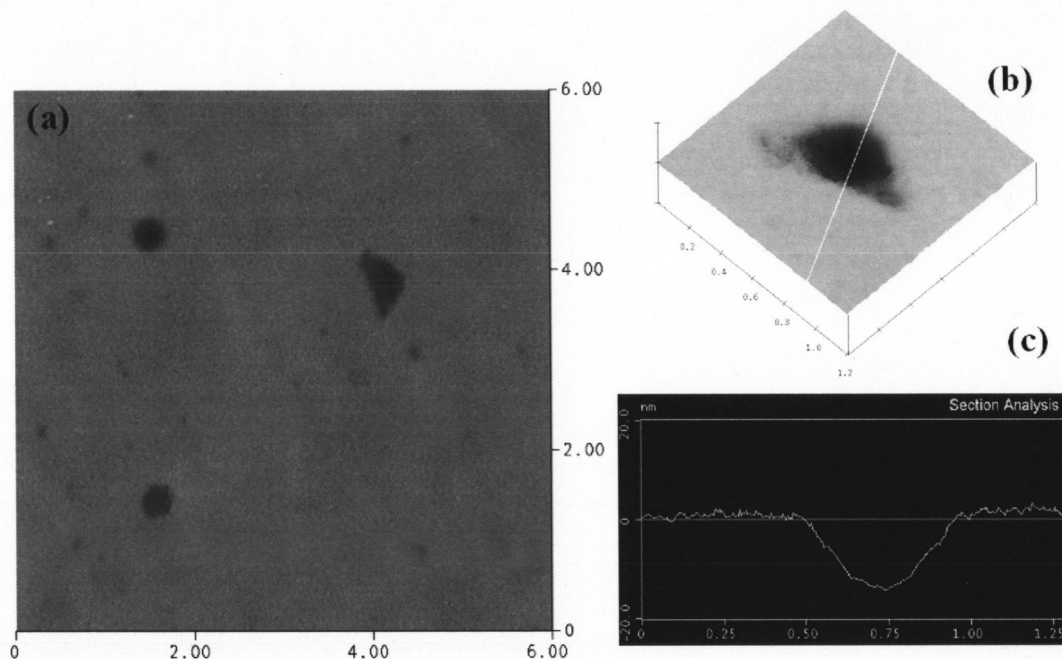


FIG. 2. (a) The AFM image from the Cu(100) surface after the methanol reduction; (b) three-dimensional AFM closer image of the indentation; (c) the cross-sectional profile drawn along the marked line in (b). The scale unit is in μm .

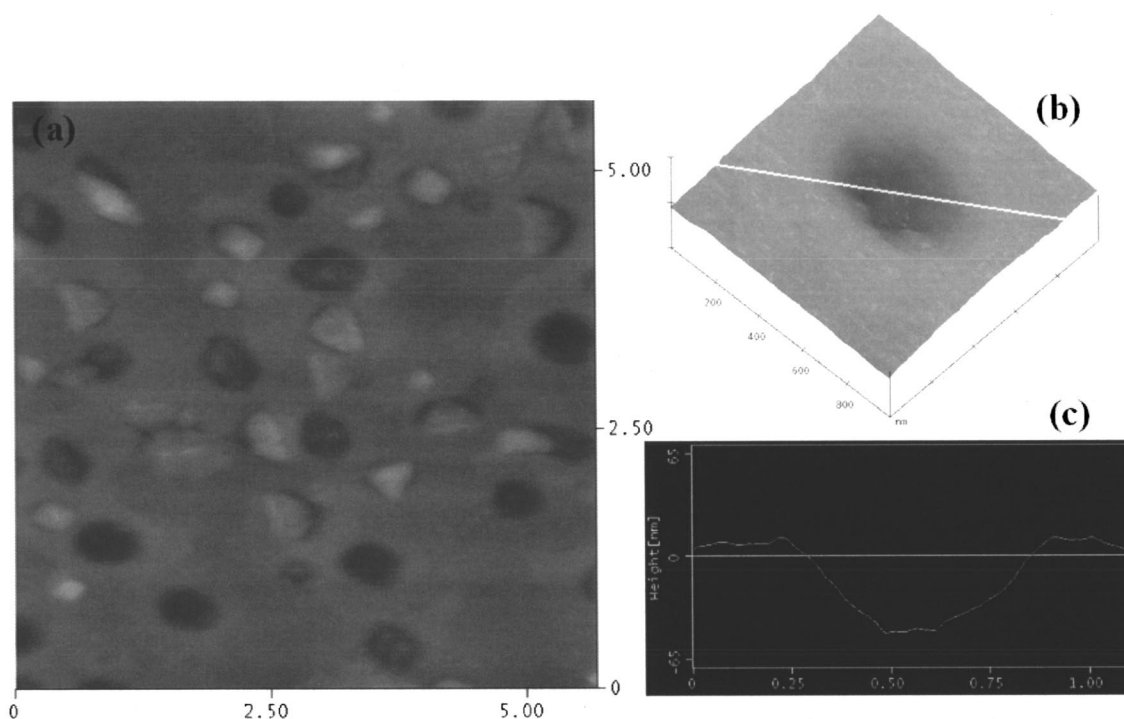


FIG. 3. (a) The AFM image from the Cu(100) surface after the second oxidation, the scale unit is in μm ; (b) three-dimensional AFM closer image of the indentation; (c) the cross-sectional profile drawn along the marked line in (b), the scale unit is in μm .

surface after the methanol reaction, i.e., corresponding to Fig. 1(a), where the Cu film was immediately cooled down to room temperature right after the methanol reduction. The areas with the dark contrast in Fig. 2(a) are the indentations, left behind when the *in situ* oxide islands were removed by the methanol reaction. Figure 2(b) is a higher magnification three-dimensional AFM image from the indentation area, where the surface of the indentation is observed to be rough. The cross-section profile of this indentation, corresponding to the marked line is plotted in Fig. 2(c). The indentation depth is ~ 12 nm, and the tilt angles of the indentation range from 5° to 15° away the film surface. No obvious faceting is observed, and it is reasonable to expect that the indentation areas have a higher density of the steps than the flat area of the Cu film. The surface topology of the Cu(100) thin film, after the second oxidation at $\sim 400^\circ\text{C}$ for 10 min, is shown in Fig. 3 and further demonstrates that the oxide islands do not preferentially nucleate at indentations. The three-dimensional higher magnification AFM image in Fig. 3(b) and the cross-section profile in Fig. 3(c) indicate that the indentations have changed shape after the second oxidation, but no significant faceting is observed. Therefore, it is still expected to have the oxide islands preferentially located at the indentation areas if the surface steps play an important role in the oxide formation. These results strongly suggest that steps at areas of locally higher surface curvature do not provide preferential nucleation site for Cu_2O islands on Cu(001).

Impurity atoms on Cu surface are possible preferential sites for oxide nucleation. Although TEM cannot image single impurity atoms, we used an indirect method to ascertain the existence of preferential nucleation sites, such as

impurities. If there were preferential nucleation sites on the copper surface due to the presence of impurity atoms, then there should be a nonuniform distribution of Cu_2O islands, but we did not observe regions with different densities of oxide islands. On the other hand, special reactive sites usually suggest zero order heterogeneous nucleation kinetics. By analogy to thin film growth, it is possible to examine the nucleation mechanism by looking at the effect of oxygen pressure on the oxide island density. If oxide formation at special reactive sites such as the impurity adsorbates or precipitates dominates, then the density of the oxide nuclei should be independent of oxygen pressure. However, our experimental observation by the *in situ* TEM clearly indicates that nucleation density varies with oxygen pressures, i.e., higher oxygen pressure leads to higher island density. We measured a decrease of the saturation density of the oxide nuclei (well before coalescence) with increasing oxidation temperature that followed an Arrhenius relationship, as is predicted for a surface-limited nucleation process.^{13,17} Therefore, we observed no clear evidence that impurities play a role in the initial formation of the oxide although there must exist some impurities on the Cu surface, even at the high vacuum conditions used in these experiments.

Another possible preferential nucleation site is at the surface termination of a threading dislocation; therefore, it is also necessary to clarify their role in the initial stages of oxidation. Figure 4(a) shows an example of the oxidation of Cu(110) film, where many threading dislocations are present. It is seen that the oxide islands have a random distribution, that is uncorrelated with the location of the dislocations.

Although we have shown that dislocations, impurities and surface steps do not play an important role in the oxide

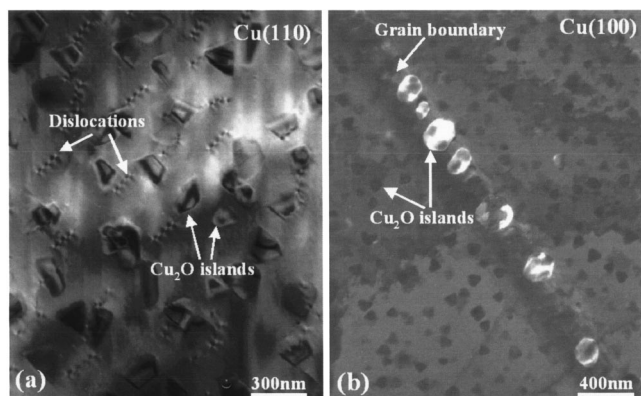


FIG. 4. (a) The oxidation of Cu(110) film with dislocations at 450 °C and oxygen pressure of 0.01 Torr; (b) the oxidation of Cu(100) film at 400 °C and oxygen pressure of 0.01 Torr, where a grain boundary is present in the film.

nucleation, extended defects such as grain boundaries do provide preferential nucleation sites for the oxide islands. Figure 4(b) shows the oxidation of a Cu(100) film containing a grain boundary. The alignment of oxide islands along the grain boundary clearly indicates that the grain boundary is the preferential nucleation site for oxide islands. Also, the larger average size of the oxide islands formed along the grain boundary indicates the oxide islands have a locally faster growth rate than the islands formed on the other area. The surface topology from the grain boundary area from AFM reveals that the grain boundaries are not grooved. We consider several physical mechanisms that may be responsible for the increase in the oxide nucleation and growth rate at the grain boundary. The most obvious mechanism would be a reduction in the nucleation energy barrier at the grain boundary due to the large number of defects along the boundary. Grain boundaries usually have high interfacial energy, which facilitates the oxide nucleation. Also, the oxygen sticking coefficient or/and the dissociation of O_2 to O at the reactive sites at the grain boundary can be enhanced. These factors would all contribute to the faster growth rate and the larger average size of the oxide islands than that formed on the single crystal surfaces.

One of the most dramatic changes a surface can undergo is faceting, where the initially flat surface changes into facets of different orientations due to thermodynamic instability at elevated temperatures or adsorption of chemical species, and it is generally believed that driving force for the faceting is the change of the surface free energy.^{18,19} We observed the faceting of the Cu(110) thin film at the elevated temperature, as shown in Fig. 5. Figure 5(a) shows the surface morphology of the Cu(110) film after methanol cleaning at ~ 450 °C, where the film has a relatively flat surface. Figure 5(b) shows surface morphology of the film after it is annealed at ~ 800 °C for ~ 40 min, where the flat Cu(110) surface becomes into a hill-and-valley structure aligned along [001] direction. The spacing between valleys or hills is ~ 300 nm in the [110] direction. When the faceted Cu(110) surface was allowed to quickly cool to room temperature, it was found the faceted surfaces do not become a completely flat surface as its initial state, it means that the surface faceting of the

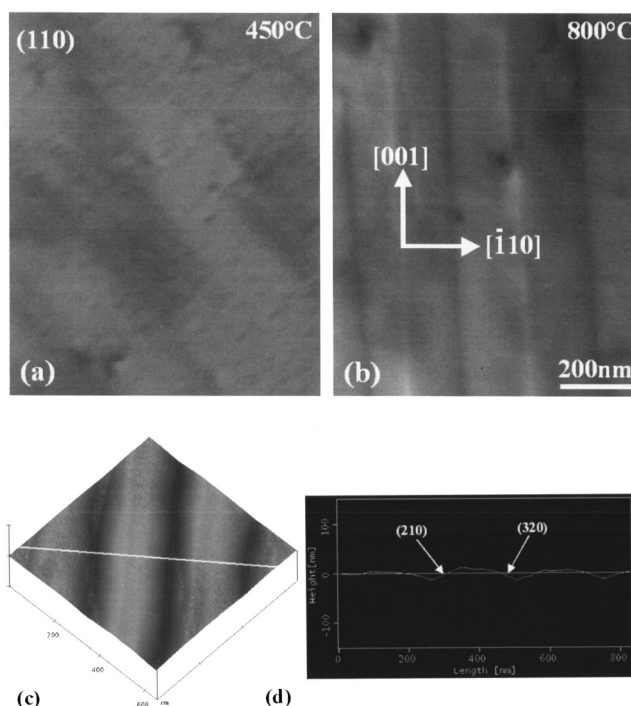


FIG. 5. The faceting of Cu(110) film at the elevated temperature. (a) Cu(110) surface annealed at 450 °C; (b) after 40 min annealing at ~ 800 °C; (c) three-dimensional AFM image of the faceted surface; (d) the cross-sectional profile drawn along the marked line in (c), and the tentatively determined facets by measuring the contact angle between the facets.

Cu(110) films in our investigation is not a completely reversible process. Observation of small copper crystals immediately below their melting point ($T_m = 1083$ °C) demonstrates that the (110) facet is absent from the equilibrium crystal shape (ECS) at this temperature.²⁰ This requires that either the (110) surface has a roughening transition at a temperature (T_R) below T_m or the (110) surface is not a stable facet at any temperature. By using surface x-ray diffraction techniques, Mochrie *et al.* have investigated the thermodynamic stability of the Cu(110) surface and demonstrated that the (110) facet of Cu is a stable equilibrium facet at low temperatures and becomes unstable (roughening or faceting transition) at higher temperatures (~ 700 °C).^{19,21} Our *in situ* TEM observation also revealed the roughening/faceting transition of the Cu(110) surfaces at \sim the similar temperatures,²² but the reversibility of the transition upon the temperature change was not observed. The possible reason for this irreversibility could be related to the fast-cooling rate of the samples and/or the particular sample geometry in our experiments. We used free standing Cu thin films (~ 800 Å) for the TEM observation. Therefore, the samples can exhibit faceting transition on both surfaces of the films, which could make the different faceting behavior of the thin films from the semi-infinite bulk samples as used in Mochrie *et al.*'s work. For a more quantitative understanding of the faceting transition of the free standing Cu(110) thin films, extensive experimental work with carefully controlled conditions and rigorous theoretical modeling are needed. The surface topology of the faceted Cu(110) was also evaluated by *ex situ* AFM as shown in Fig. 5(c). Cross-sectional analysis using the AFM was performed

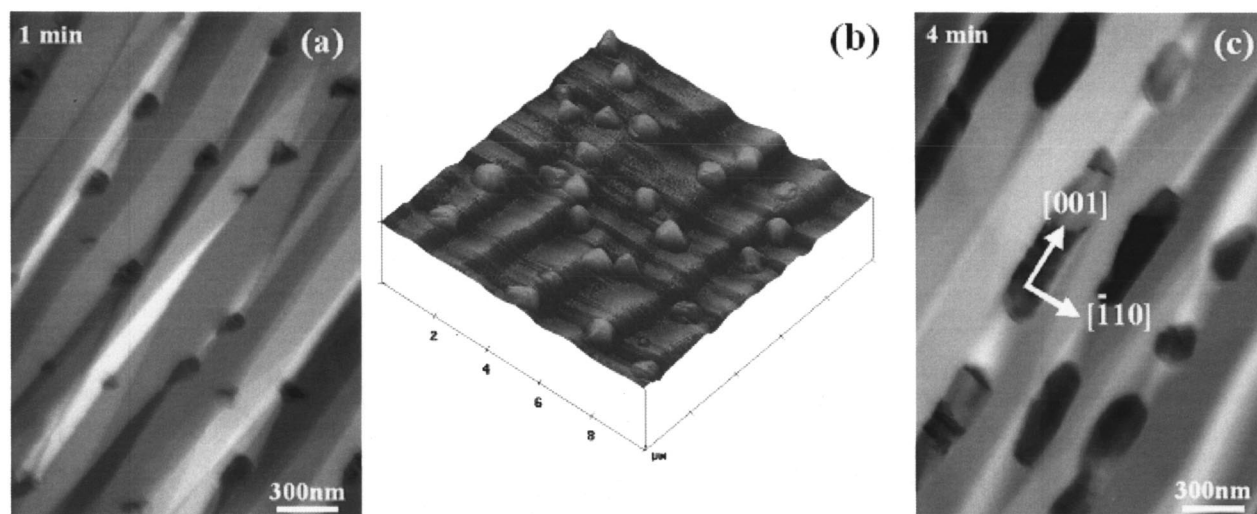


FIG. 6. The oxidation on the faceted Cu(110) surface at $\sim 800^\circ\text{C}$. (a) The preferential nucleation of the oxide islands at the facet corners; (b) the three-dimensional AFM image from the oxidation of the faceted Cu(110) surface; (c) the preferential growth of the oxide islands along the intersection direction, [100], of the facets with the continuous oxidation.

in order to measure the contact angles between the neighboring facets. From the crystallographic direction, [100], of the line defined by the intersection of the two facet planes, the contact angle allows the facets to be tentatively indexed. The marked line in Fig. 5(c) is parallel to [110] direction, and the corresponding cross-section surface profile is plotted in Fig. 5(d). The contact angle between the normal to the facet and the [110] direction was measured to be $\sim 11^\circ$ and $\sim 18^\circ$ by using the cross-sectional profile line. The facets were determined to be $\{210\}$ and $\{320\}$, as shown in Fig. 5(d).

Figure 6 shows the oxidation of a faceted Cu(110) surface by leaking oxygen into the TEM column at $\sim 800^\circ\text{C}$ and the oxygen pressure of 5×10^{-4} Torr, where the facet corners are observed to be the preferential sites for oxide nucleation. This preferential nucleation at the facet corners is further confirmed by the AFM image as shown in Fig. 6(b), where most of the islands are located at the facet corners, including both the bottom and the crest of the corners. The continuous oxidation of the faceted Cu(110) surface results in the preferential growth of the oxide islands along the intersection direction, as shown in Fig. 6(c), where the islands are elongated and aligned each other along the [001] direction. The nucleation of oxide islands at the bottom of the facet corners can be easily understood in terms of a reduction in the change in interfacial energy. While the preferred nucleation at the crests cannot be explained in this way. Perhaps there are some other mechanisms to control the nucleation of oxide islands at the crests, and the line energy associated with the corners could play an important role in the oxide formation at these locations. It has been reported that vicinal surfaces are used for fabricating magnetic wires by epitaxial growth methods.^{23–25} Similarly, the faceted surfaces provide the hill-and-valley structures that could be used as templates for fabricating oxide nanostructures, as shown here.

Typical substrates in real experimental systems are not perfectly flat, and contain many surface steps, ledges, dislocations, etc. In thin film growth and formation of self-

assembled nanostructures, the impact of imperfections need to be considered, such as in the comparisons between experimental data and theoretical simulations.^{26,27} In the present work, we created the different surface defect structures on copper films and systematically examined their effects on oxide nucleation and growth for copper films with different orientations. Our observations indicated that surface defects such as steps, impurities and dislocations are relatively unimportant in the initial formation of oxide, thus, oxide nucleation appears to be homogeneous. Therefore, in the theoretical treatment of the initial stages of oxidation of metals, the effects of surface defects on the nucleation of oxide islands need not to be considered. However, three-dimensional defects such as grain boundaries and large surface changes, such as surface faceting, were observed to provide preferential nucleation sites and growth directions. The observation from the *in situ* oxidation of the faceted Cu(110) surfaces suggests that faceted surfaces could be used as templates for patterning oxide island arrays and growing one-dimensional oxide nanostructures.

IV. CONCLUSIONS

The effects of the surface topology on the oxide formation in the initial stages of oxidation of Cu films were investigated by an *in situ* UHV-TEM and *ex situ* AFM. Our experimental observation indicates that 3D oxide nucleation occur homogeneously, and dislocation and surface defects steps do not play a significant role in the initial formation of oxide. On the other hand, grain boundaries (when present) can provide preferential nucleation sites and enhanced growth rates for oxide islands. The *in situ* observation of the oxidation on faceted Cu(110) surfaces reveals that the corners between two facets are the preferential nucleation sites for oxide islands and the oxide islands show a quasi-one-dimensional growth along the these facet corners.

ACKNOWLEDGMENTS

This research project is funded by NSF (No. 9902863) and National Association of Corrosion Engineers (NACE)—Air Force Office of Scientific Research (AFOSR) seed grant. The experiments were performed at the Materials Research Laboratory, University of Illinois at Urbana-Champaign, which is supported by the U.S. Department of Energy (No. DEFG02-96-ER45439). The authors kindly thank I. Petrov, R. Twesten, M. Marshall, and K. Colravy for their help.

- ¹G. Dujardin, A. J. Mayne, G. Comtet, L. Hellner, M. Jamet, E. Le Goff, and P. Millet, *Phys. Rev. Lett.* **76**, 3782 (1996).
²F. M. Ross and J. M. Gibson, *Phys. Rev. Lett.* **68**, 1782 (1992).
³G. Dujardin, F. Ross, and A. J. Mayne, *Phys. Rev. Lett.* **82**, 3448 (1999).
⁴A. J. Mayne, F. Ross, and G. Dujardin, *Surf. Sci.* **523**, 157 (2003).
⁵P. H. Holloway and J. B. Hudson, *Surf. Sci.* **43**, 141 (1974).
⁶S. Zalkind, M. Polak, and N. Shamir, *Surf. Sci.* **513**, 501 (2002).
⁷W. X. Huang, R. S. Zhai, and X. H. Bao, *Appl. Surf. Sci.* **158**, 287 (2000).
⁸K. Heinemann, D. B. Rao, and D. L. Douglas, *Oxid. Met.* **9**, 379 (1975).
⁹R. H. Milne and A. Howie, *Philos. Mag. A* **49**, 665 (1984).
¹⁰J. C. Yang, M. Yeadon, B. Kolasa, and J. M. Gibson, *J. Electrochem. Soc.* **146**, 2103 (1999).
¹¹M. L. McDonald, J. M. Gibson, and F. C. Unterwald, *Rev. Sci. Instrum.* **60**, 700 (1989).
¹²J. C. Yang, M. Yeadon, B. Kolasa, and J. M. Gibson, *Appl. Phys. Lett.* **70**, 3522 (1997).
¹³G. W. Zhou and J. C. Yang, *Surf. Sci.* **531**, 359 (2003).
¹⁴G. W. Zhou and J. C. Yang, *Appl. Surf. Sci.* **222**, 357 (2004).
¹⁵G. W. Zhou and J. C. Yang, *Phys. Rev. Lett.* **89**, 106101 (2002).
¹⁶G. W. Zhou and J. C. Yang, *Appl. Surf. Sci.* **210**, 165 (2003).
¹⁷J. C. Yang, M. Yeadon, B. Kolasa, and J. M. Gibson, *Scr. Mater.* **38**, 1237 (1998).
¹⁸W. W. Mullins, *Philos. Mag.* **6**, 1313 (1961).
¹⁹B. M. Ocko and S. G. J. Mochrie, *Phys. Rev. B* **38**, 7378 (1988).
²⁰K. D. Stock and E. Menzel, *Surf. Sci.* **61**, 272 (1976).
²¹S. G. J. Mochrie, *Phys. Rev. Lett.* **59**, 304 (1987).
²²G. W. Zhou and J. C. Yang, *Surf. Sci.* **559**, 100 (2004).
²³S. Rousset, V. Repain, G. Baudot, H. Ellmer *et al.*, *Mater. Sci. Eng., B* **96**, 169 (2002).
²⁴D. Spisak and J. Hafner, *Phys. Rev. B* **65**, 235405 (2002).
²⁵C. T. Yu, D. Q. Li, J. Pearson, and S. D. Bader, *Appl. Phys. Lett.* **79**, 3848 (2001).
²⁶J. A. Venables, G. D. T. Spiller, and M. Hanbuecken, *Rep. Prog. Phys.* **47**, 399 (1984).
²⁷C. Ratsch and J. A. Venables, *J. Vac. Sci. Technol. A* **21**, S96 (2003).